8th Biennial International Conference
& Exposition on Petroleum Geophysics

"HYDERABAD 2010"

P-133

Data Conditioning, Curvature Analysis, and Spectral Decomposition Processing of 3-D Data

Charles Blumentritt, Dr. Rahul Das Gupta, Mr. Sibam Chakraborty*, Mr. Asheesh Singh*

Summary

We processed a stacked, migrated volume from a 3-D survey through our data conditioning software and created a substantially improved conventional trace volume which greatly reduced noise and improved continuity of reflections. This data set allowed the Client to more accurately locate faults and generate locations to exploit "attic" oil. The improved data set was available for additional post-stack processing including volumetric curvature and spectral decomposition.

Introduction

A series of oil and gas fields have been discovered in the Deohal-Burdubi Area (Figure 1) form Oligocene Barail and Langpar Sandstone in the Assam Arakan basin, onshore NE India (Oil India Ltd, 2008). The post stack processing was carried out in a 3-D seismic survey which consists of 117 lines of 341 traces each with a trace spacing of 25 m and a line spacing of 50 m for a total coverage of 50 km^2. Each trace consists of 1251 samples with a 4 ms sample interval for a total trace length of 5.0 seconds. The original data was very noisy and generally lacking in reflections that are continuous over large lateral distances. It is also possible or likely that such areas indicate that migration of the seismic data did not fully collapse the diffractions originally in the data. Nevertheless, the evidence for such faults occurs above and below the apparently continuous reflections and on closely spaced parallel lines or crosslines.

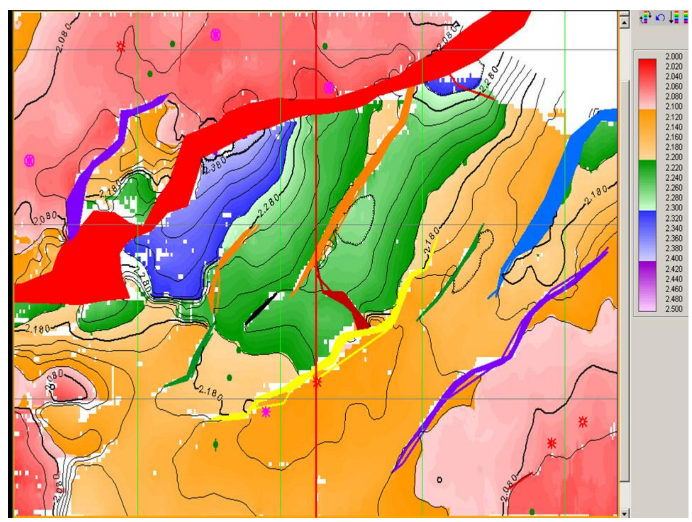

Figure 1. Time structure map for representative horizon.

Interpretation Methodology

Principal Component Analysis: Prior to any curvature analysis and spectral decomposition, we applied our Principal Component Analysis (PCA) conditioning to the data set. Our data conditioning algorithm is essentially a three dimensional dip filtering routine which uses the multi-dimensional matrix algebra of principal component analysis to determine the best fit surface at each sample of the volume. Although the analysis is done in three dimensions, the multi-dimensional plotting becomes impossible to draw, so we will illustrate the process with two dimensional diagrams. The process uses a small sub-volume of the data, usually 3 lines by 3 traces by 11 samples, around the sample being analyzed. Figure 2 shows a series of traces which have been transformed through a Hilbert Transform into the energy domain (Green Shading and red line). The sub-volume is indicated by the blue crosses, indicating the energy values for each of the samples.

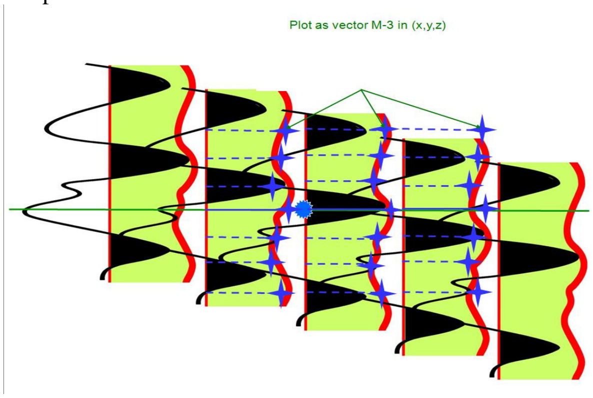

Figure 2. Two dimensional representations of seismic traces. Green shading and red line indicate traces transformed into the energy domain. Blue circle indicates sample being analyzed. Blue stars and dashed lines represent energy values of specific samples in the three dimensional sub-volume used for the principal component analysis.

Each level of the sub-volume may be plotted as a vector in 9+ dimensional space, where each dimension represents the energy value of on the traces in the sub-volume (Figure 3).

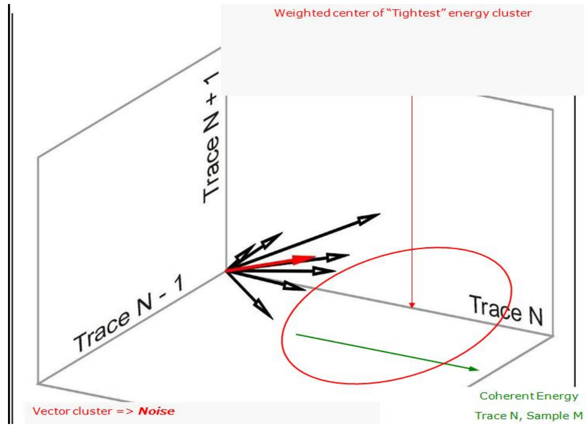

Figure 3. Vector plot of sub-volume in Figure 2. For each dip in a series of dip scans, the vectors form a cluster and the "tightest" cluster represents the optimum surface at that sample. The weighted center of that tightest cluster is projected back to the axis of trace being analyzed and put out as the "conditioned" data.

In a perfect case, all of the vectors would be co-linear and the cluster represents noise. The process is repeated for each dip in a series of dip scabs and the dip which produces the tightest cluster indicates the dip of the surface at that sample. As long as the seismic reflections are continuous, a multi-trace filter can produce good results. However, when this is some kind of discontinuity in the data, a multi-trace filter may smooth out any such breaks (Figure 4). To overcome this problem, we use a Kurahawa filter to produce preserve the breaks.

The process described above is repeated for a sub-volume centered about each of the traces in the original sub-volume. The position which produces the tightest cluster is used for the sample at the center of the original sub-volume.

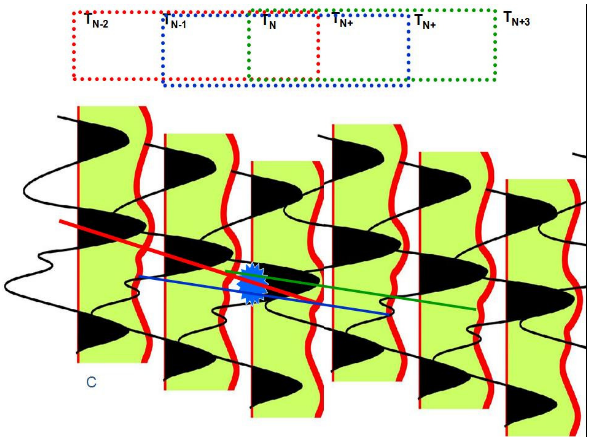

Figure 4. Kurahawa filter. In the case of a break in the data, an analysis made at the location of the blue circle would produce an inferior result. In this case, the analysis is repeated for a sub-volume centered around each trace in primary sub-volume. An analysis centered on the right hand trace (green) would produce a result similar to the one centered around the middle trace. However, an analysis centered on the left trace (red) would produce a superior result.

Figure 5 shows a seismic line from this survey as indicated on the map. Section of the left is from the original data and the section of the right is after conditioning. The conditioned section shows substantially less random noise and significantly more continuity along the reflections. The sub-vertical brown lines indicate faults whose locations are poorly imaged in the original data, but are precisely locate on the conditioned data.

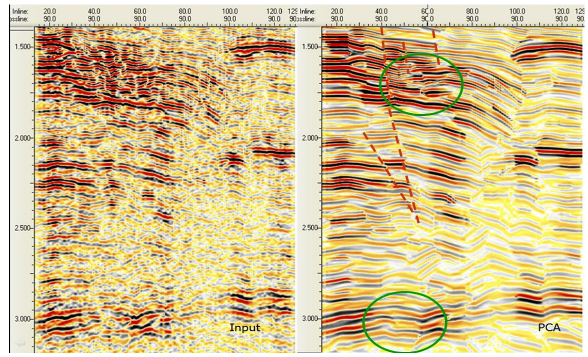

Figure 5. Seismic line indicated in Figure 4. PCA conditioned data shows substantial decrease in noise and increased continuity of reflections; see especially areas in green circles. The dashed brown lines represent faults which are poorly imaged or not visible on the original data.

Figure 6 shows the mapped horizon at the target level. Autopicking is possible of the conditioned data and the map shows very well the track of the fault. Such a result may be useful for determining reserves and additional locations. Figures 7 and 8 show the input and PCA conditioned data from a line indicated in Figure 8. On the original data, the position of the fault separating Well C from Wells A and B is very poorly defined. After PCA conditioning, the position of the fault is very clear and indicates that there is some updip potential between Well C and the fault.

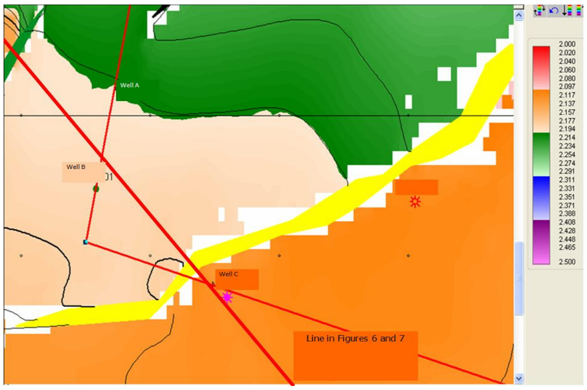

Figure 6. Structure map showing the line Figure 7 and 8 and the positions of Wells A, B, and C. Note the well defined position of the fault up dip of Well C.

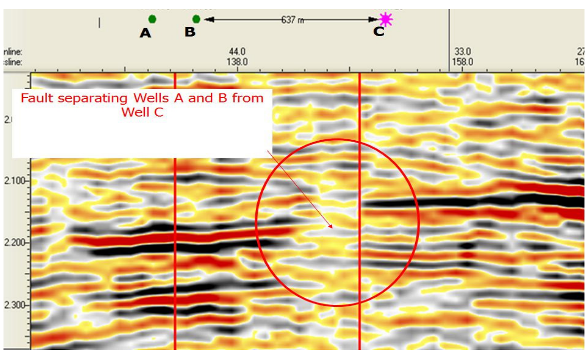

Figure 7. Line connecting two producing areas as shown in Figure 6. Data is from the original input survey.

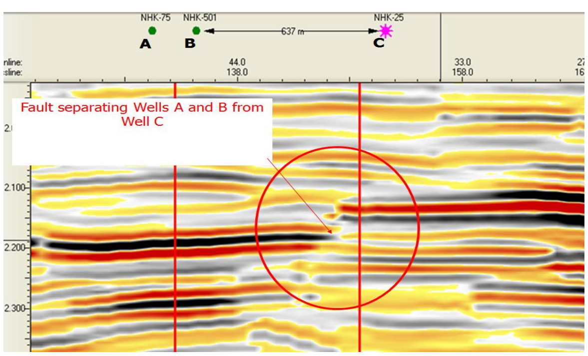

Figure 8. Same line as Figure 7 from PCA conditioned data set. The trace of the fault is well defined in this display which will provide a better delineation of the reservoir.

Curvature Analysis: After PCA processing we computed the curvature on the same data set. Curvature is a two dimensional property computed along a single azimuth of a surface. To understand this, it is easiest to consider a 2-D profile (Figure 9). Along this profile, the dip changes forming different types of folding. At each point along this profile, there is one and only one tangent circle. In areas of concave downward (anticlinal) folding, the circles are below the surface and, in cases of concave upward (synclinal) folding, the circles are above the surface. Each of these circles has a radius, with tighter circles having smaller radii. Curvature has two simplistic definitions: the rate of change of dip and the inverse of the radius of the tangent circle. By convention, we assign positive values of curvature to anticlinal folding and negative values of curvature to synclinal folding.

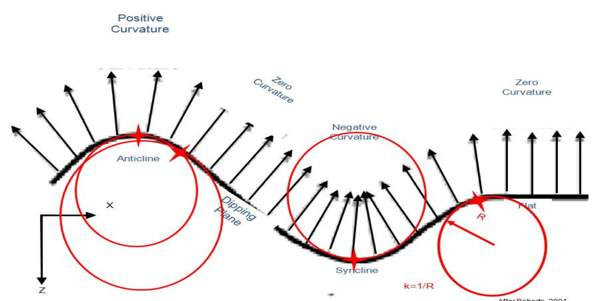

Figure 9. Curvature in two dimensions. At each point along a profile, there is one and only one tangent circle. As the folding gets tighter, the size of the tangent circle and its corresponding radius (R) get smaller. Curvature (k) may simply be understood as the inverse of this radius, so that tight folding corresponds to greater curvature. By convention, anticlinal folding corresponds to positive values of curvature and synclinal folding corresponds to negative values.

In three dimensions, there are a large number of azimuths about to compute the curvature at any given point P (Figure 10). For any second order Surface, there are two principal curvatures: the Maximum Curvature, which represents the plane in which the folding is the tightest and the Minimum Curvature, which represents the plane in which the folding is the broadest. These two planes are perpendicular. Additional curvatures are those which are computed in the dip direction and in the strike direction.

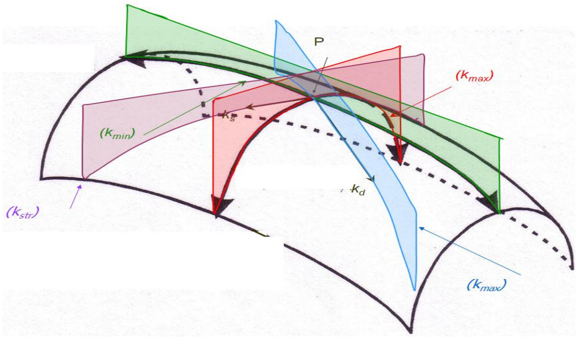

Figure 10. Curvature in three dimensions. For a surface there are two principal curvatures: Maximum Curvature, k_{max}, which defines the tightest curvature and Minimum Curvature, k_{min}, Additional obvious curvatures include the curvature measured in the dip direction, k_{dio}, and the curvature measured in the strike direction, k_{str}.

Two additional non-intuitive curvatures are the Most Positive and the Most Negative Curvatures (Figure 11). Maximum Curvature refers to magnitude and may be positive or negative. Most Positive and Most Negative Curvatures are similar to Maximum Curvature, except that they highlight anticlines and synclines, respectively. In the case of a saddle, with the folding tightest in anticlinal direction, Maximum Curvature will show the anticline and truncate the syncline. Most Positive Curvature will show the anticline only. Most Negative Curvature, however, will show the entire syncline. For this reason, Most Positive and Most Negative Curvature highlight anticlines and synclines, respectively, to a greater degree than Maximum Curvature. Curvature is a property of a surface and software has been developed to compute curvature along gridded surfaces, such as interpretation of 3-D seismic data create. However, there are sometimes problems with such surfaces during interpretation.

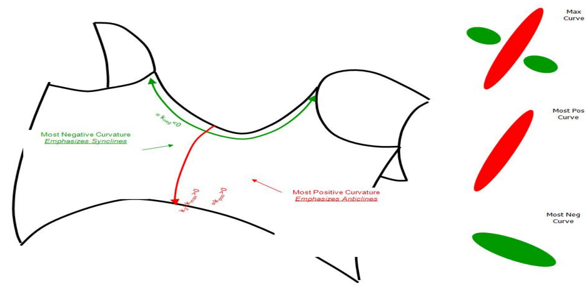

Figure 11. Most Positive/Most Negative Curvature. Maximum Curvature shows the greatest magnitude of folding, regardless of polarity. Most Positive Curvature highlights anticlines and Most Negative Curvature highlights synclines.

During our PCA conditioning process, we use the sub-volumes to compute well behaved surfaces for every sample in the full volume. We then calculate curvature for every sample in the full volume so that we can overcome any problems with horizon interpretation. In fact, it is easily possible to view the results along time slices.

Figure 12 shows the Most Positive and Most Negative Curvatures for a time slice at 2.2 seconds within the data volume with lineaments identified on them.

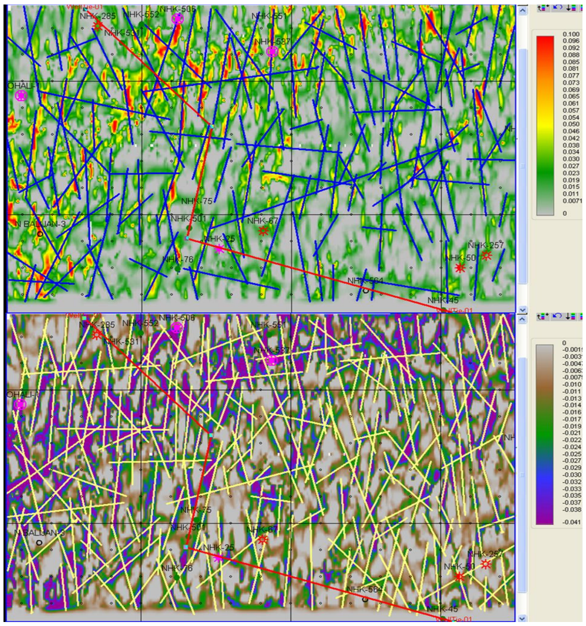

Figure 12. Most Positive Curvature (Upper) and Most Negative Curvature (Lower). Blue and yellow lines represent lineaments which have been identified and whose orientations are shown in Figure 13.

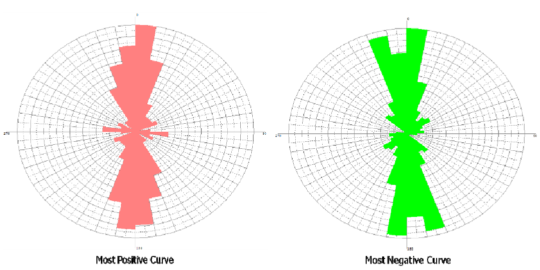

Figure 13. Orientations of lineaments in Figure 12.

As a casual inspection would indicate, the predominant trend on both of these displays is generally north to south (Figure 13). Figure 14 shows three possible tectonic origins for such preferred orientations: east-west extension, north-south compression, and north-northeast to south south-southwest left lateral wrenching.

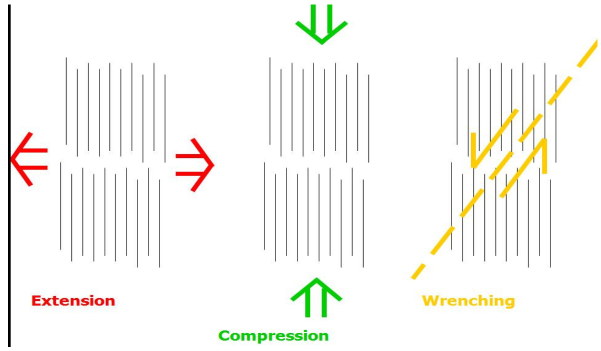

Figure 14. Possible explanations for north-south trending lineaments.

Figure 15 shows a time slice from the basement in which an anticlinal trend crosses the slice from east to west with offsets in the middle. An interpretation of this slice indicates northeast-southwest left lateral wrench faulting.

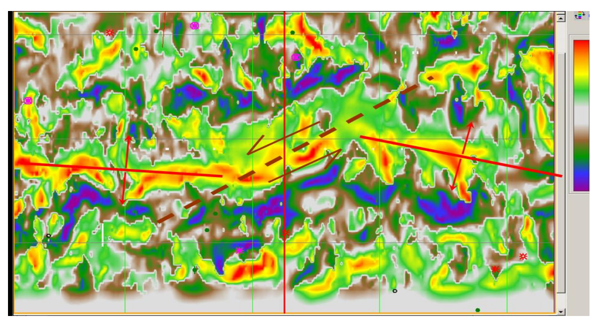

Figure 15. Maximum Curvature, Time slice 3.188 (Basement). Anticlinal trend shows changes in orientation corresponding to northeast-southwest left lateral wrench faulting. Trends in the sedimentary section (Figures 13 and 14) are consistent with this model.

Spectral Decomposition Highlight Volumes: Spectral decomposition is the process of breaking down seismic traces into the component sine waves which may be summed for form the trace. Normal processing for spectral decomposition produces one volume of amplitude response for each frequency analyzed, and variations in amplitude by frequency for a various area are generally believed to be related to stratigraphic variations. This results in a large number of volumes to be interpreted. We provide what we call Highlight Volumes (Figure 16) which summarize the information in those numerous individual frequency volumes. For each sample in the volume, we compute an amplitude spectrum.

On this amplitude, there is some frequency (Peak Frequency) at which the spectrum reaches a maximum (Peak Amplitude). Time or horizon slices of this maximum amplitude are often similar to amplitude slices from the original trace volume. To locate anomalous areas, we subtract the average for each individual spectrum from the maximum. If the result is a low number, then the spectrum is relatively flat. If the result is large, the peak value for this sample is truly anomalous.

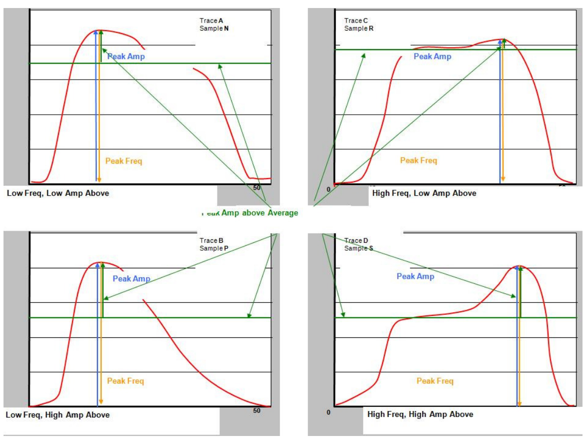

Figure 16. Highlight volumes. This diagram represents amplitude spectra for four generic samples in a volume. At each sample, there is a frequency (Peak Frequency) for which the spectrum reaches a maximum (Peak Amplitude). To determine if this Peak Amplitude is anomalous or not, we subtract the average for the spectrum from the peak to produce the Peak Amplitude above Average. Large values indicate anomalous results and small values indicate flat spectra.

Figure 17 shows a map of Peak Amplitude Above Average for the horizon shown in Figure 8. Wells A and B are productive, but Figure 6 indicates that they are not structurally controlled. This attribute indicates that the production may be associated with stratigraphic features.

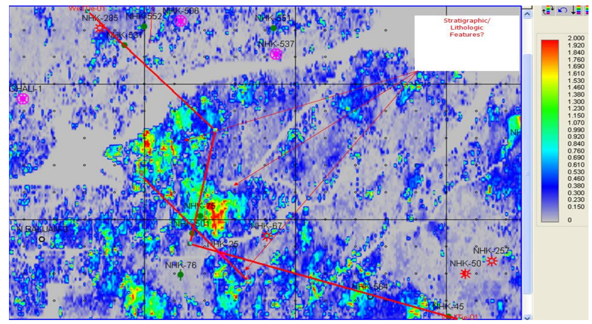

Figure 17. Peak Amplitude Above Average (PAAA). Wells A and B (Figure 6) are not on structural closure, but have produced hydrocarbons. PAAA shows that the production may be related to a stratigraphic body outlined by this attribute.

Conclusion

Our conditioning process is very powerful at reducing noise and improving continuity. In this case, the combination of data quality along with presence of short segments of continuous data results in areas in which faults may cross apparently continuous reflections. With Principal Component Analysis (PCA) and achieved substantial improvement in data quality.

In this case, there is a great deal of structural variability within the survey. Interpretation of the curvature volumes suggest that the area is dominated by right lateral wrench faulting in the basement. Within the Oligocene zone, there is a preferred orientation of lineaments representing subtle anticlines, synclines, faults, and flexures with a narrow lateral extend oriented in a north-south direction a more northeast-southwest for structures with a broader lateral extent.

Our spectral decomposition highlight volumes suggest that depositional stratigraphic trends with a north-south to northwest-southeast orientation may be present within that same zone. Spectral decomposition highlight volumes indicate that wells which produce in an area which is not structurally closed may be related to a stratigraphic body.

Acknowledgments

The author gratefully acknowledges Mr Vickram Ghorpade (President, Suvira Group) for his constant support & encouragement throughout the work. Special thanks goes to Mr. Mark Stevenson (Director- Geotexture Technologies Houston) for his help & motivation for compiling this abstract with his tremendous upstream petroleum expertise and support. Finally, the E&P world will take a significant seismic leap forward with the use of the Geo-texture Technologies Interpretation services which is logical to learn and deploy in E& P activities to interpret sub surface better. With more than 1,000 customers all over the world, Geo-texture is truly the global industry leader for Data Conditioning, Curvature analysis and Spectral Decomposition.

References

Bergbauer, S., T. Mukerji, P. and P. Hennings, 2003, Improving curvature analyses of deformed horizons using scale-dependent filtering techniques, AAPG Bulletin, V. 87, No. 8, pp. 1255-1272

Blumentritt, C. K. J. Marfurt, and E. C. Sullivan. 2006, Volume based curvature computations illuminate fracture orientations, Geophysics in press.

Hart, B. S., Pearson, R., and Rawling, G. C., 2002, 3-D seismic horizon-based approaches to fracture-swarm sweet spot definition in tight-gas reservoirs: The Leading Edge, 21, 28-35.

Marfurt, K., 2005, Robust Estimates of 3D reflector dip and azimuth, Geophysics, in press.

Masafero, J.L., M. Bulnes, J. Poblet, and N Casson, 2003, Kinematic Evolution and Fracture Prediction of the Valle Morado Structure inferred from 3-D seismic data, Salta province northwest Argentina, AAPG Bull., v. 87, no. 7. pp. 1083-1104.

Roberts. A., 2001, Curvature attributes and their application to 3D interpreted horizons, First Break, 19 85-100.

Sigismondi, M. E., and Soldo, J. C., 2003, Curvature attributes and seismic interpretation: Case studies from Argentina Basins, The Leading Edge, 23, 1122-1126.